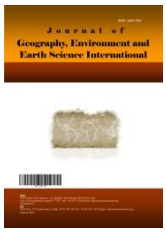

Journal of Geography, Environment and Earth Science International

24(1): 45-62, 2020; Article no.JGEESI.54504
ISSN: 2454-7352

Small Scales Dynamics Inferred from Tidal Measurements to Mitigate Daily Floodings in the City of Douala: A Case Study of the Besseke's Flood Drain

Besack Felix[1,2*], Onguene Raphael[3], Ebonji Seth Rodrigue[1,2], Oben Mbeng Lawrence[1,2], Kouandji Bekoumb Joseph Betsaleel[2], Sone Essoh Willy[2] and Tomedi Eyango Minette[1,2]

[1]Institute of Fisheries and Aquatic Sciences, University of Douala, Yabassi, Cameroon.
[2]Laboratory of Fisheries and Aquatic Resources, University of Douala, Cameroon.
[3]Douala Institute of Technology, University of Douala, Cameroon.

Authors' contributions

This work was carried out in collaboration among all authors. Authors BF and OR designed the study and wrote the protocol. Authors BF, KBJB and TEM performed the statistical analysis and wrote the first draft of the manuscript. Authors BF, SEW and ESR managed the analyses of the study and the literature searches. All authors read and approved the final manuscript.

Article Information

DOI: 10.9734/JGEESI/2020/v24i130193
Editor(s):
(1) Dr. Azza Moustafa Abdel-Aty, Department of Water Pollution Control, Environmental Division, National Researcher Center, Egypt.
Reviewers:
(1) Moses Oghenenyoreme Eyankware, Ebonyi State University, Nigeria.
(2) Jianhui Yang, Henan Polytechnic University, China.
Complete Peer review History: http://www.sdiarticle4.com/review-history/54504

Original Research Article

Received 06 December 2019
Accepted 12 February 2020
Published 14 February 2020

ABSTRACT

The recently constructed Besseke's flood drain is always filled with water due to individual or combined effect of the tide, urbanization drainage, underground plumes and precipitations runoffs. This study focused on the analysis of small scales dynamics inferred from short term tidal measurements to mitigate the daily flooding in the Besseke's flood drain. The methodology used is based on field measurements observation. The sampling of water level was conducted during two (02) different tidal regimes in May 2019. The volume of brackish water moving in and out of the Besseke's flood drain was calculated using the formula of O'Brien. The results showed that Spring

**Corresponding author: E-mail: besackocean@gmail.com;*

conditions had greater amplitudes than Neap tide conditions. During Spring tides, the tidal prism that passed in the midsection of the Besseke's flood drain (S4) was 3.5×10^1 m^3. This means that only a negligible amount of the incoming brackish water reaches the Besseke's flood drain, amplifies and causes the daily flooding. The unexpected stronger amplitudes and dynamics observed in S4 could be due to its sub estuary nature. Furthermore, the percentage composition of water in this section, showed that the fraction of brackish water changes from 85.7% during Spring tide to 77.8% in the Neap tide conditions. The overall spatial evolution revealed that, the trend in tidal prism (during Spring conditions) was (S0) > (S2) > (S1) > (S3) > (S4) with corresponding values of 2.1×10^4, 1.3×10^4, 1.0×10^4, 2.5×10^2 and 3.5×10^1 m^3 respectively. Finally, Tidal prism and Cross-sectional area showed a perfect correlation ($r^2 = 0.96$). The best fitted Cross-sectional area-Tidal prism relationship was obtained in S3 (Market) during Spring tide condition.

Keywords: Small scales dynamics; tidal prism; cross-sectional area; Besseke's flood drain and Wouri estuary.

1. INTRODUCTION

Drainage and flood control problems in many urban regions are directly linked to human interference with normal drainage patterns [1]. In many growing coastal cities, drainage solutions are in three basic directions; anticipatory, preventive and remedial works. These solutions can be structural or non-structural depending on the objectives and actions. Basically, as urbanization proceeds, adequate local drainage should be provided along with streets, roads, schools, parks, public and private facilities. If the drainage system is not properly handled, remediation activities will be inevitable. Today, special actions of flood warnings (remedial) and flood insurance are being installed and developed in modern cities. In the same way, urban drainage and flood control activities require an assessment of the benefits derived by those being relieved of potential flood damages. In many cases, urban storm drainage is of great necessity because of the advancing urbanization of these areas couple to the continuous sea-level rise.

Storm surges are the main driver of coastal flooding leading to loss of human life, destruction of homes and civil infrastructures, disruption of trade, fisheries and industry [2]. The variability of these types of risks depends on the level of exposition and degree of vulnerability of the population. The impacts of a storm surge may further intensify when it coincides with high spring tide [3] and/or riverine flooding [4]. Many flood risks assessments have treated these two drivers independently in coastal regions [5]. Other Authors such as [6] have also investigated the interaction of storm-tide and riverine flooding drivers in the Lee estuary using a coupled ocean-hydrodynamics model. Zheng et al. [4] observed statistically significant dependence between extreme rainfall and storm surge residuals along the east coast of Australia and advised to consider both processes jointly to correctly quantify flood risk. Many studies have shown that floods management require an evaluation of existent risks, their spatial variability as well as their frequency of occurrence [7]. It can also be concluded that populations of many gauge estuaries and rivers confronted to flood risk have mainly three options, resisting, retreating and adaptation depending on the nature and intensity of the flood event [8].

In Cameroon, studies related to floods events have not yet been properly handled, the only existing documents are focused on coastal areas like Douala. This coastal city is the economic capital of the country (Cameroon) and bears 75% of the industrial units, 62% of the national income and 45% of employment [9]. It is also the most populated city with about three (03) million inhabitants [9]. This growing population is expected to double to six (06) million by 2035 [9]. Despite its economic and commercial importance, this economic headquarter faces numerous environmental problems like saltwater intrusion and floods of all types including marine submersions at different temporal and spatial scales. A recent study shows that flood disasters are now quasi annual, more intensive and more severe with central points along river Wouri [10]. This is mainly due to its location in an estuarine zone were the altitude is relatively low with near-surface groundwater [11] and [12]. To reduce or prevent floods and their impacts, several measures have to be taken by the various stakeholders. In Douala, the local authorities and researchers (The University of Douala) have invested on important environmental projects

such as the large drainage project initiated by the Douala Urban City council (D.U.C) since the years 2000. The main aims of this project was to drained water from different neighbourhoods into the Wouri estuary. This project was reinforced by the JEAI-RELIFOME cooperation in 2015, that investigated the response of the Cameroon coastline to multi-scale ocean forcing's. Another project was the Douala Secondary City in 2017 that aimed to map potential flooding areas and mitigate flood events in the city and finally the Douala sustainable city project in 2018 with its main objective of increasing resilience of the city towards floods events and climate change impacts. Despite the sufficient documentation of tidal processes along the Wouri estuary especially in its lower section [13] the upper section bearing the Besseke and Bonaberi neighbourhoods remains poorly investigated. However, the construction of dykes, embankments and flood drains have been the main floods resistance and mitigation infrastructures in this section and by the year 2019, a total of about 40 km of flood drain was constructed out of the expected 250 km in the concerned neighbourhoods of Douala.

The Besseke's flood drain project constructed to drain the Bessecke's watershed is instead permanently overfilled with brackish water. Because of this situation, its construction remains uncompleted. Knowledge on how the water in the flood drain interacts with various tidal regimes, couple tidal and weather conditions and drained water from urbanization were not handled with care during the designing and construction operations of the flood drain. The unsatisfactory results obtained in the case of the besseke's flood drain projet has raised many questions on the efficiency of flood control by these infrastructures in the coastal city of Douala.

The Cameroon estuary (Wouri estuary) experiences a semi-diurnal tidal regime and for this reason, urban drainages and flood control systems (flood drain) that drain water generated from urbanization should accommodate with additional sea or brackish water (tidal prism) from the main Wouri estuary. Unfortunately, this aspect has not been adequately evaluated throughout the planning, programming, design-ing and construction activities related to the Besseke's neighbourhood project (flood drain construction). This article, therefore, investigates the small scale features of tidal parameters and discusses the process of the tidal prism evolution around the Besseke's flood drain during two differents tidal regimes, adopting the combined method of empirical formula and field data measurements. This will serve as a tool to evaluates the performances of the flood drain through the use of linear regression analysis between morphological and hydrological parameters [14].

1.1 Presentation of the Study Ground

The city of Douala occupies about 18 000 hectares of land with a population of about 3 million inhabitants [9]. The Besseke's zone is an area of particular interest in this large watershed. A great part of this zone is considered below the mean sea level during Spring tide conditions. Our area of interest is positioned at the saline intrusion limit (oligohaline) or limnique part of the Wouri estuary (a character that depends on the seasons and tidal regime). Looking at the astronomical, bathymetric and atmospheric conditions, the tidal regime in this section may range from micro (amplitude less than 1 meter) to macro tidal (amplitude greater than 3 meters). According to Olivry [15] and Olivry [16], tides in the lower section of Wouri estuary are semi-diurnal and very asymmetric. Like most watershed in the country, the Besseke presents a dumping area for the population and consequently containe zones of pollutants accumulation in its lower section.

Since the last decade, this city is experiencing continuous urbanization resulting in the anthropisation and denaturation of its aquatic environment. This is shown by the intense land reclamation along the wouri estuary accelerated wetlands and swamps occupation. This area is also characterized by uncontrolled land occupation unable to respect the urbanization plan of the Douala City Council.

The recently constructed Besseke's flood drain is always filled with water due to individual or combined effect of the tide, urbanization drainage and precipitations. It is a tidally dominated, fluvial influenced or mixed tidal-fluvial regime dominated region. The Besseke's flood drain and the Wouri estuary where it empties itself are presented in Fig. 1.

2. MATERIALS AND METHODS

2.1 Duration of the Study and Sites Selection

The data used in this study were collected in May 2019 (Dry season with low river flow),

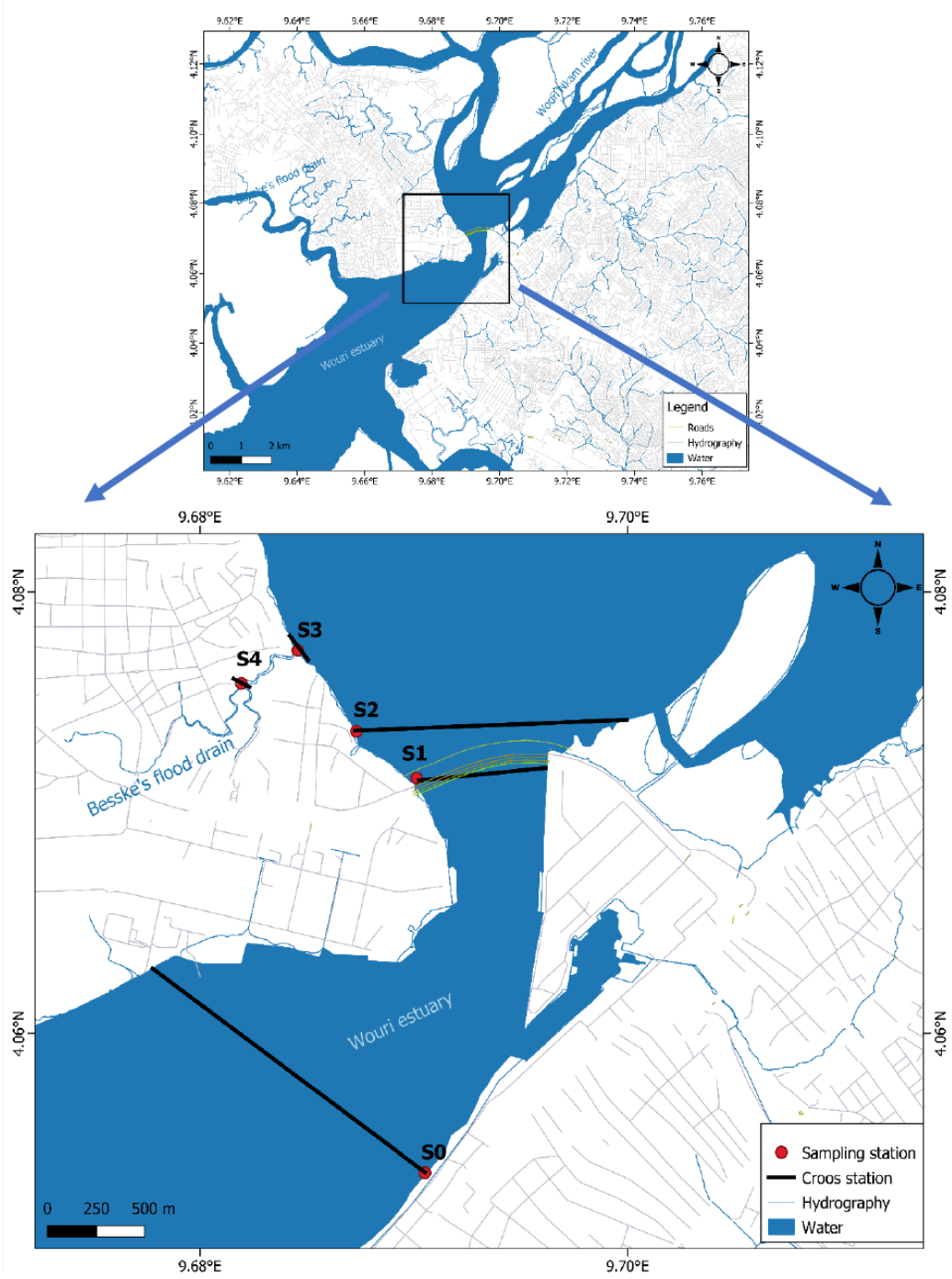

Fig. 1. Presentation of the study ground

during two different tidal coefficients. The first sampling period with a tidal coefficient of 52 was on May 11, 2019 (corresponding to a Neap tidal regime) while the second period was on May 18, corresponding to a Spring tide conditions. Five (05) sampling/gauging stations were installed along the upper section of the Wouri estuary (Fig. 1). Their reference field names and geographic positions are shown in Table 1.

These sampling stations were chosen according to their accessibilities, existences of tidal records installations and security. Other specific factors shown below were also taken into consideration;

S0: The pressure sensor station of the Douala harbour (Fig. 2). This station is about 50 km away from the open Atlantic ocean.

S1 : Near the bonaberi bridge, very dynamic zone with small eddies.
S2 : The Besseke's market, about 1 km from S0, with a relatively large cross-section.
S3 : The entrance of the Besseke's flood drain with a smaller section due to the size of the drain. This station is about 2 km away from S0.
S4 : Midpoint of the Besseke's flood drain. It is a junction point between the two branches of the flood drain and is located about 3 km from S0. All these sampling stations are well illustrated in Fig. 1 of the presentation of the study ground.

Table 1. Description and location of sampling stations

Code	Station	Longitude	Latitude
S0	Douala harbour (SM4)	9.6909	4.5370
S1	Bonaberi bridge	9.6902	4.0712
S2	Bonassama market	9.6881	4.0742
S3	Drain inlet (entrance)	9.6850	4.0772
S4	Mid drain section at Besseke	9.6819	4.0750

2.2 Data Collection/Acquisition System

2.2.1 Water elevation

A short-term sampling of water level was conducted during two (02) different tidal regimes in May 2019. Five sampling stations were established along the Besseke's flood drain and the surrounding Wouri estuary (Fig. 1). In each gauging station, the water height was recorded every fifteen-minutes (15 mins) time intervals and this was done for at least half of the duration of a complete tidal cycle (12 hours 42 minutes). These measurements were conducted simu-ltaneously at a synchronized recording time. Due to limited finance to purchase tide gauges or an acoustic doppler current profilers (ADCP), tide rods were used to measure the water level in S1, S2, S3 and S4. The only available tide gauge (pressure sensor) was found in S0 (Douala harbour) and it's data were made available by the port authorities. The sampling principle of the pressure sensor in S0 is presented in Fig. 2. The average 12 methods were used to correct the missing data. The following parameters are presented in Fig. 2.

2.2.2 Geometric and hydrologic parameters

A flying-boat was used for cross-shore displacement and the distance travel (width) across each sampling station was determined using a Global positioning system (GPS). The Depth in S0 and S1 were determined using simulations of the hydrodynamic model SYMPHONIE. On the other hand, a graduated scale bar of Seven (7) meters long was used to estimate the depths in the other sampling points (S1 to S4). During these bathymetric operations, (three) 03 transects were considered (from one shore to another) in each station and the mean depth was determined. This was done during low and high water slakes of the two tidal conditions investigated. These parameters further help in the computation of the cross-sectional area (Equation 2), discharge (equation 3) and tidal volume (equation 1, modified to 15 minutes). All

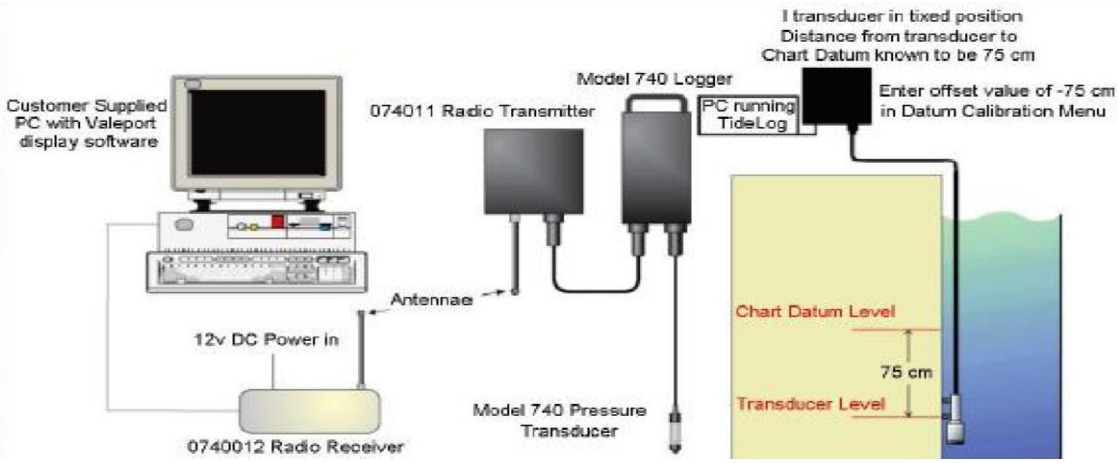

Fig. 2. Schematic of the measurements system of water elevation in the Douala harbour (S0)
(Source : [13])

these formulae have been proposed by Marcel and Rakhorst [17]. During high/low water slakes, salinity was also recorded in S4 only using a multi-parameter of brand HORIBA.

To identify and characterize small-scale features of tidal parameters in the Besseke flood drain and it surrounding Wouri estuary, different parameters were analyzed. This leads to the computation of secondary data. The most important secondary data (parameters) involved in this investigation were cross-sectional area, tidal prism, small scale discharge (sinusoidal discharge) flow velocity and salt fraction.

2.3 Computation of Secondary Data

Tidal prism : The tidal prism is the amount of water that flows in and out of an estuary or bay with the flood and ebb of the tide, excluding any contribution from freshwater inflows [18]. It can also refer to the volume of the seawater that an estuary or a bay can take in within an average tidal range condition [19]. The discharge method (equation 1) was used to calculate this parameter. This method was chosen as it seems to provide a better fit than other methods.

$$\boldsymbol{P} = \boldsymbol{\Delta H} \times A \quad (1)$$

In this equation, P is the tidal prism, ΔH is the tidal elevation and A is the cross-sectional area.

The cross-sectional areas (A): Care should be taken as they are arranged in the estuary to record the inward and outward flux during one tidal cycle [19]. The gauging consisted of three transversal depth measurements across each of the gauging stations. The average depth was also measured during different tidal conditions. Equation 2 was used for the calculation of cross-sectional areas (A).

$$A = \boldsymbol{C} \times \boldsymbol{D} \quad (2)$$

With C as the cross-section width and D being the average depth at a particular time.

Sinusoidal discharge: The discharge due to the tidal prism is an important parameter in the study of small scales. The method used for the calculation this parameter was similar to the US army corps method [20] that relates tidal prism with discharge during a tidal cycle (equation 3). This equation was modified to extract 15 minutes processes.

$$Q = \frac{\pi P}{T} \quad (3)$$

Where Q is the discharge flow, P representing the tidal prism, T the tidal period (taken as 900 seconds for small scale computation) and π is a constant.

Characteristic flow velocity: An estimation of the tidal prism velocity is calculated from the relationship between tidal prism, cross-sectional area and tidal period (Equation 4).

$$u = \frac{2P}{AT} \quad (4)$$

Where u is the tidal velocity, P (m cube) as a tidal prism, A (m square) representing the cross-sectional area and T (sec) the tidal period (usually 12.42 hours for the semi-diurnal period).

Salt fraction: The salt fraction in the water was computed to estimate the percentage composition of brackish water at each station. This enables us to know the amount of water from the Wouri estuary that enters the Besseke's flood drain during a semi tidal period. The computation of the salt fraction was done using equation 5.

$$Fs = \frac{s_L}{s_n} \times 100 \quad (5)$$

Where Fs is the Salt fraction, SL the measured salinity and Sn representing the salinity of the ocean or the nearest ocean point.

Cross-sectional vs Tidal prism empirical relation (A-P relationship): The widely recognized relationship between cross-sectional area (A) and tidal prism (P) was initially established by Leconte [21] and later by O'Brien [22,23]. Jarrett [24] furthered increase the understanding of this relationship by grouping inlets into separate classes based on wave energy setting and the presence or absence of jetties.

Although many authors had developed a different relationship between the tidal prism and cross-sectional area (A-P relationship), we have considered the familiar empirical relationship (equation 6) of O'Brien [23] for this study.

$$A = \boldsymbol{a} \cdot \boldsymbol{P^n} \quad (6)$$

Where A (m^2) is the cross-sectional area at equilibrium, P (m^3) is the tidal prism corresponding to the astronomical tidal range, a and n are coefficients (empirical parameters). These coefficients were calculated using the method developed by Marcel and Rakhorst [17].

2.4 Statistical Analysis

Pearson correlation coefficient was used to determine the correlation between cross-sectional areas and tidal prisms. Small scale variation in tidal parameters was also computed to observed high frequency [mean time of fifteen minutes (15 mins)] variabilities of the various parameters along the different stations displayed in the study ground (Fig. 1). The computation and curves visualization were done using the Matlab (Matrix Laboratory) R2013a (8.1.0.604) version.

3. RESULTS

The primary objective of this research was to characterized the evolution of small-scale features of tidal parameters along the region of freshwater influence and analyzed them in terms of spatial and temporal scales using field measurements from tide rodes and pressure sensor. This section reports the results of the study and it has focused principally on small-scale features along the Besseke flood drain and the upper section of the Wouri estuary.

3.1 Tidal Signal

A systematic analysis of water levels was done from Douala harbour (S0) to the middle part of the Besseke flood drain (S4), passing through the Bridge (S1), Market (S2), and Drain inlet (S3) (Fig. 1). The results of this analysis were presented in the marigrams of Fig. 3 (A and B) below. The amplitudes obtained during Spring tide conditions (Fig. 3A) were 1.18, 1.23, 1.01, 0.96 and 1.18 m representing S0, S1, S2, S3 and S4 respectively. These amplitudes were reduced during Neap tide conditions (Fig. 3B) to corresponding values of 0.97, 0.88, 0.66, 0.57 and 0.9 m. It can again be observed that the tidal signal is semi-diurnal with a longitudinal variation of hypersynchronous (from S0 to S3) and hypersynchronous (S3 to S4) properties. Finally, the result also suggested that the tidal wave travels from S0 to S4 in about one (1) hour during a Spring tide (Fig. 3B) and about 1 h 30 mins during Neap tide condition (Fig. 3A).

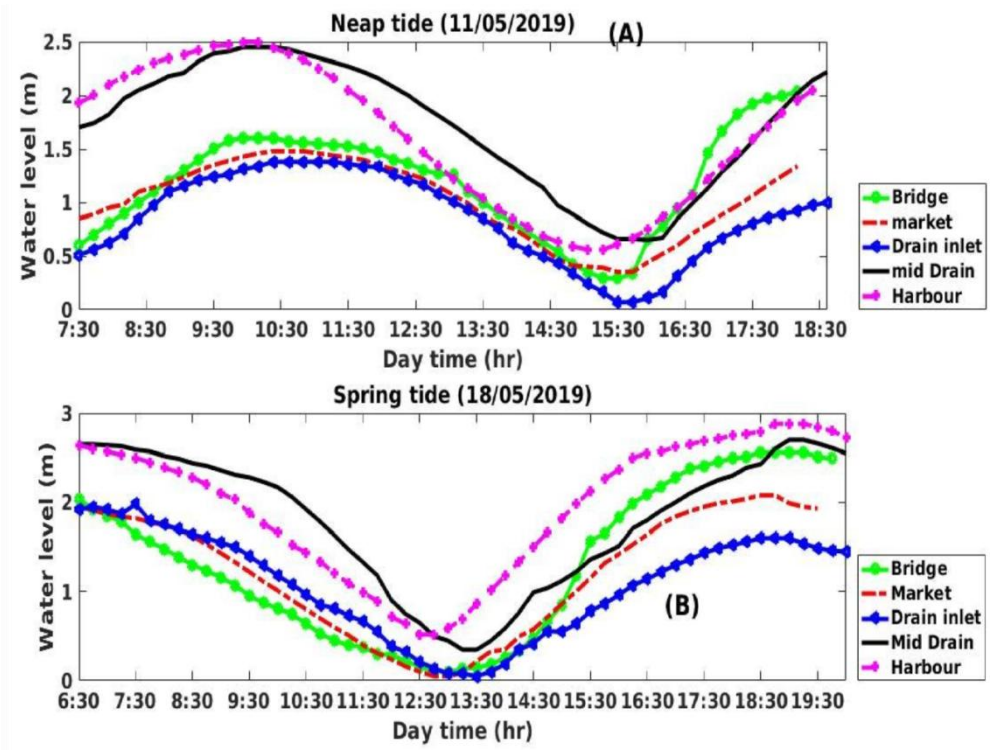

Fig. 3. Propagation of tidal wave from S1 to S4 showing distortion properties. The pink broken line =Daouala habour (S0), green=Bridge (S1), red=market (S2), blue=drain inlet (S3) and black=mid drain (S4)

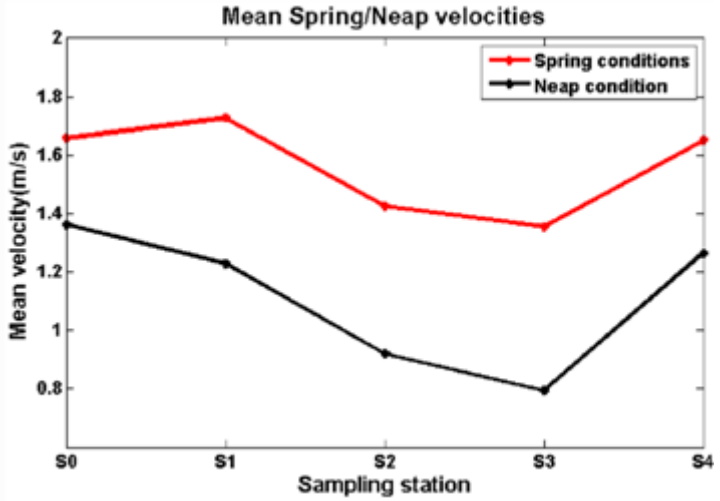

Fig. 4. Evolution of tidal velocities during spring and neap tidal regimes. The red line shows spring tide velocities while black line accounts for neap conditions velocity

3.2 Flow Velocity Distribution

The Flow velocity is an important parameter, use in the understanding of the tidal distortion and tidal prism dynamics. After the analysis of the tidal signal, the displacements of water particles was examined. The means flow velocities with which water particles travel across the different sampling stations during Spring or Neap tide regime were calculated from equation 4. The results of these computations (Fig. 4) showed that Spring conditions had relatively higher velocities compared to Neap tide condition. During Spring situation, velocities decrease from S0 to S3 with values of 1.65, 1.75, 1.50 and 1.40 m/s representing S0, S1, S2 and S3 respectively. In S4, this velocity is instead increased to 1.8 m/s.

A similar trend was observed during the Neap tide regime, with values of 1.38, 1.25, 0.9, 0.8 and 1.35 m/s representing S0, S1, S2, S3 and S4 respectively.

3.3 Small Scale Tidal Dynamics

To understand the daily flooding of the Besseke's flood drain, a 15 minutes (900 seconds) time interval of small scales features of water level were extracted and presented in Fig. 5. The negative values represent Ebb tide current while the positive values portray Flood current situation (filling with water). The length of the bars represents the elevation intensities. When observing the small scale elevations during the two tidal conditions, It was noticed that Spring conditions (red bars) had relatively higher amplitudes (stronger perturbations) compared to those of Neap tide conditions (blue bars). Focusing on the daily trends, the peak values observed during Spring current were found around 04:30 pm (16 h:30 mins in French) while those of Neap condition appears two (02) hours later (06:30 pm). Looking at the spatial scale, the trend in this peak values was Bridge (S1) > Mid drain (S4) > Harbour (S0) > Market (S2) > Drain inlet (S3) with values of 0.45, 0.2, 0.18, 0.17 and 0.17 m respectively. This trend in small scale features (peak values/15 mins) was maintained during neap tide conditions but with relatively smaller intensities. Stability in small scales can also be observed at different periods in each station, This is the case in the Bridge (S1) from 6:30 to 8:30 am during flood current (positive blue bars).

3.4 Tidal Prism Dynamics

Due to Flood or Ebb currents conditions, the area of shoals was not the same, leading to differences in the tidal water areas (tidal volumes). The tidal prism, discharge volume and the parameters used for their estimation are presented in Table 2. Generally, the tidal range, discharge volume and tidal prism decrease gradually from S0 to S3. Some exception to this trend is found in S1, during Spring tide (tidal range) and in S2 during both tidal regimes (tidal prism). Regarding tidal prism, the results obtained also showed that Spring tide had relatively higher tidal prisms than their corresponding Neap tide conditions. At spatial

scale, the tidal prisms passing through S0, S1, S2, S3 and S4 during Spring tide conditions were 2.1×10^4, 1.0×10^4, 1.3×10^4, 2.5×10^2 and 3.5×10^1 m^3 respectively. When comparing these values with their corresponding Neap tide condition, the percentages decrease were -19%, -31%, -38.5%, -48% and -48.6% accounting for S0, S1, S2, S3 and S4 respectively. Indeed, the total tidal prism that passes in the Besseke's flood drain during the Spring tide regime was 3.5×10^1 m^3. This value represents only 0.16% of the tidal prism (2.1×10^4 m^3) entering in the Douala harbour (S0) during the same tidal cycle. This percentage is again reduced to 0.11% during the Neap tide condition.

3.5 Dilution/mixing in the Besseke's Flood Drain

The objective was to investigate the dynamics of brackish-fresh water passing through this flood drain. The percentage composition of water in the Besseke's flood drain (S4) was determined using equation 5. This was performed in S4 only because of its proximity to the population of the Besseke neighbourhood. The results obtained (Table 3) show that during Spring tide the percentage composition of brackish water in the drain was about 85.7% while that from underground plumes and urbanized freshwater from homes and industries was only 14.29% (Table 3). During Neap tide, the volume of brackish water that travelled and enters the Besseke's flood drain dropped to 77.8%. In the same manner, the urbanized freshwater from homes, industries and possible underground flow increased to 22.2%.

3.6 Small Scale Features of Water Discharge

This section aims to characterized small-scale daily discharges and played a crucial role in the understanding of water transport in and out of the Besseke's flood drain, and brings out the potential tidal effects [25].

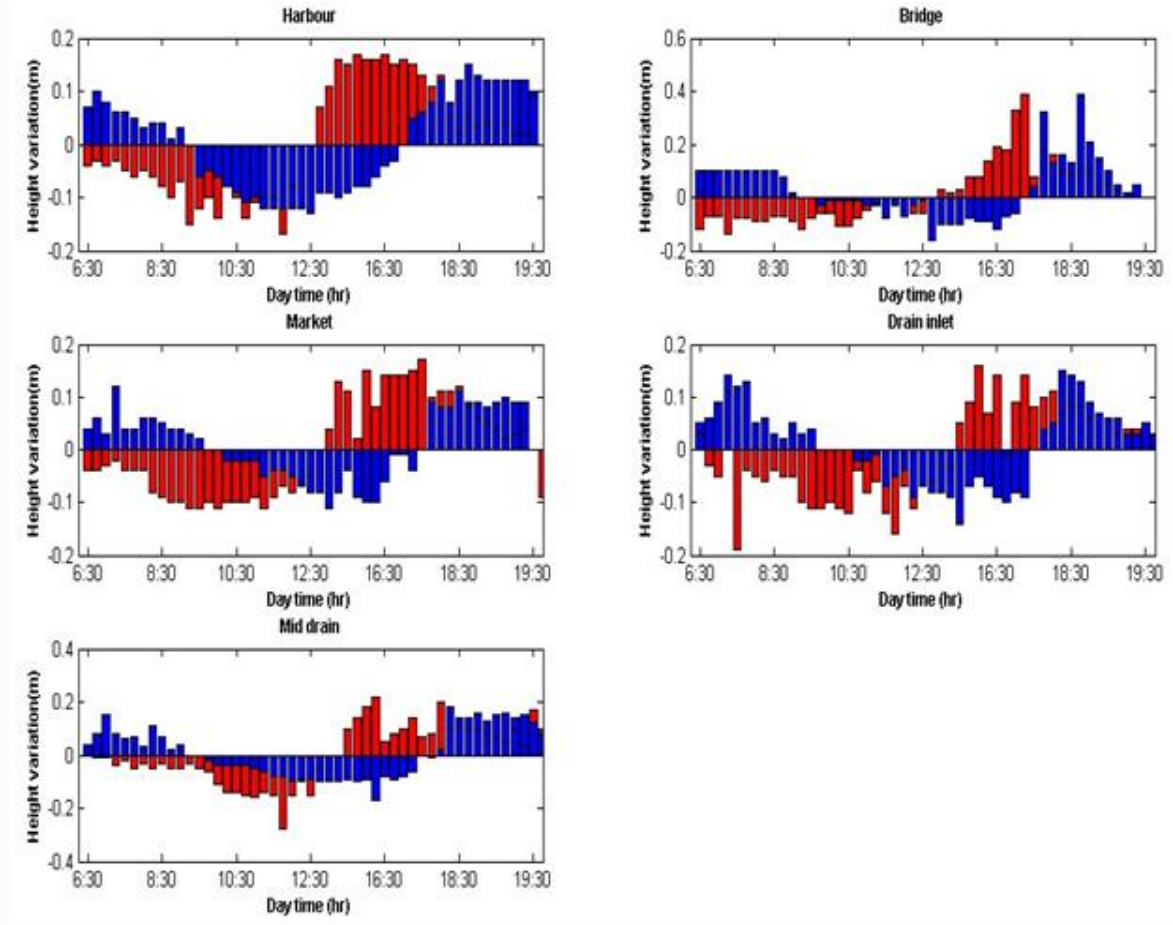

Fig. 5. Small scales evolution of tidal dynamics in the five (05) sampling stations. Red and blue bars represent Spring and Neap conditions respectively

Table 2. Computed tidal parameters from field measurements

Tidal conditions	Sampling stations	High water levels (m)	Low water levels (m)	Tidal ranges (m)	Cross-sectipnal areas (m^2)	Tidal discharges (m^2/s)	Tidal prisms (m^3)
Spring tide	S0	2.88	0.52	2.36	8877	1.4716	2.1×10^4
	S1	2.56	0.10	2.46	4151	0.7173	1.0×10^4
	S2	2.08	0.05	2.03	6540	0.9326	1.3×10^4
	S3	1.98	0.05	1.93	128	0.0174	2.5×10^2
	S4	2.70	0.35	2.35	15	0.0025	3.5×10^1
Neap tide	S0	2.50	0.56	1.94	8657	1.1798	1.7×10^4
	S1	2.04	0.29	1.75	3955	0.4862	6.9×10^3
	S2	1.48	0.17	1.31	6160	0.5669	8.0×10^3
	S3	1.38	0.25	1.13	112	0.0089	1.3×10^2
	S4	2.45	0.65	1.80	10	0.0013	1.8×10^1

Table 3. Percentage composition of water in the Besseke flood drain

Tidal regimes	Salt fractions	Percentage composition of brackish water (%)	Percentage composition of fresh water (%)
Spring tide condition	2.4/2.8	85.7	14.3
Neap tide condition	2.1/2.7	77.8	22.2

By using the measurements of Spring and Neap tide conditions in May 2019, the small scales (15 mins time interval) tidal discharge in the Wouri estuary and the Besseke's flood drain were calculated using equation 4. The negative values indicate that the direction of flow is downward (outward) while the positive sign indicates an upward directions (filling). The variability in spatial intensities of small scale features of water discharge during Spring condition (Fig. 6) showed a decreasing trend from S0 to S4. The estimated peaks vales of small scales features of tidal discharge during flood current of Spring conditions were 2000, 1500, 1000, 20 and 05 m^3/15 mins, accounting for S0, S1, S2, S3 and S4 respectively. Similarly, The peak values during Ebb current of spring conditions were -1000, -500, -700, -21 and -2.1 m^3/15mins. At this point, a small inversion in trend was noted between S1 and S2 (-500 and -700 respectively). Looking at the daily dynamic, it was noticed that the peak values (positive) appear between 14:00 and 15:30, just one hour (1 hr) before high water slakes.

During Neap tidal regime (Fig. 7), the peak value of small scales traversing each gauging station during flood current were 1200, 3000, 800, 18 and 1.8 m^3/15 mins. Similarly, the volume of water passing in an inverse direction during Ebb current were -1000, -1000, -200, -15 and -1.5 m^3. The above order accounts for S0, S1, S2, S3 and S4 respectively. During both Spring and Neap tides, the peak values appear just about one hour (1 hr) before high water slake while the least values occur before low water slakes.

Looking at the intertidal conditions (Spring-Neap tides), the small scale values obtained during Spring tides were relatively higher than their corresponding Neap tide values (Exception in S2). The spatial evolution showed that the peak value obtained during Spring tide was founded in the Harbour (2000 m^3/15 mins) and migrated to the Bridge (3000 m^3/15 mins) during Neap tide condition.

3.7 Relationship between Hydraulic (Tidal Prism) and Morphological (Cross-Sectional Area) Parameters (Empirical Formulations of A-P relationship)

This theoretical A-P relationship is only valid for a set of inlets or estuaries with similar values of littoral drift, sediment diameter, water density, tidal periods and river flow [26,27]. These phenomenological processes were considered constant in this study; only the tides and cross-sectional area were found to be changing.

After the calculation of both tidal prism (P) and cross-sectional area (A), a graph of the results obtained from equation 6 was plotted (Fig. 8) to investigate the relationship between these two parameters.

The result firstly reveals a perfect correlation (r^2 = 0.96) confirming a strong interdependency

between these parameters. The coefficients **a** and **n** calculated from this relationship (equation 6) were 3.40 $\times 10^{-2}$ and 0.46 respectively. These values are in the range of those obtained by Powell et al. [28] for medium longshore transport systems, where a = 1.2 $\times 10^{-2}$ and n = 0.69.

The deviation of black solid circles from the bleu straight line characterized sections above and below the equilibrium relation of O'Brien [23]. This relationship was applied here as preliminary guidance for the evaluation of physical conditions; station above the equilibrium (i.e. mostly neap tide periods at Harbour, Bridge and Market) were qualified as depositional while those below the equilibrium (Drain inlet and Mid drain) were characterized as erosional [29]. The lowest tidal prism (< 0.5×10^4) were found in S3 (drain entrance/inlet) and S4 (Besseke's flood drain). Even though these values were the lowest, the deviations they presented indicated that the volume of water passing in these sections was slightly higher than the equilibrium. Indeed, the cross-sectional area at S3 and S4 were slightly lower than as predicted by the equilibrium of O'Brien [23] during the Spring and Neap tide conditions. A similar observation was done in the S0 and S1 sections during Spring tide. Paradoxically, during Neap tide condition, the S2 and S0 have cross-sectional areas that were greater than equilibrium.

Finally, the Market showed the best fit to the O'Brien relationship during Spring tide [22,23].

4. DISCUSSION

In the presentation of the results, the study was the focus in describing the daily flooding features, their variability and trends. These parameters were characterized in both temporal and spatial scales. In this section, we will discuss how the small-scale features presented could be suitable in studying the filling of a flood drain. Related processes encounter will also be examined here.

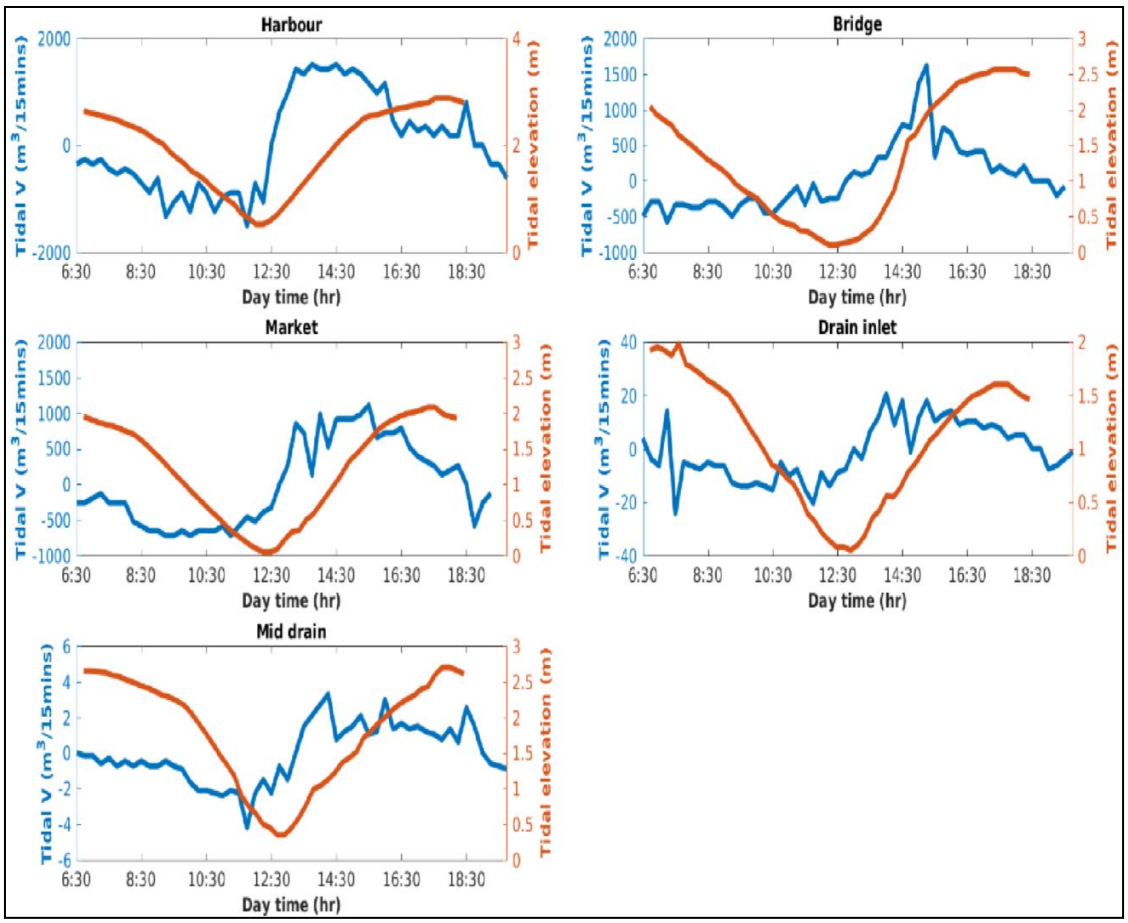

Fig. 6. Evolution of small-scale features of water discharge with alongside water level of spring tide condition. harbour, bridge, market, drain inlet and mid drain representing S0, S1, S2, S3 and S4 respectively

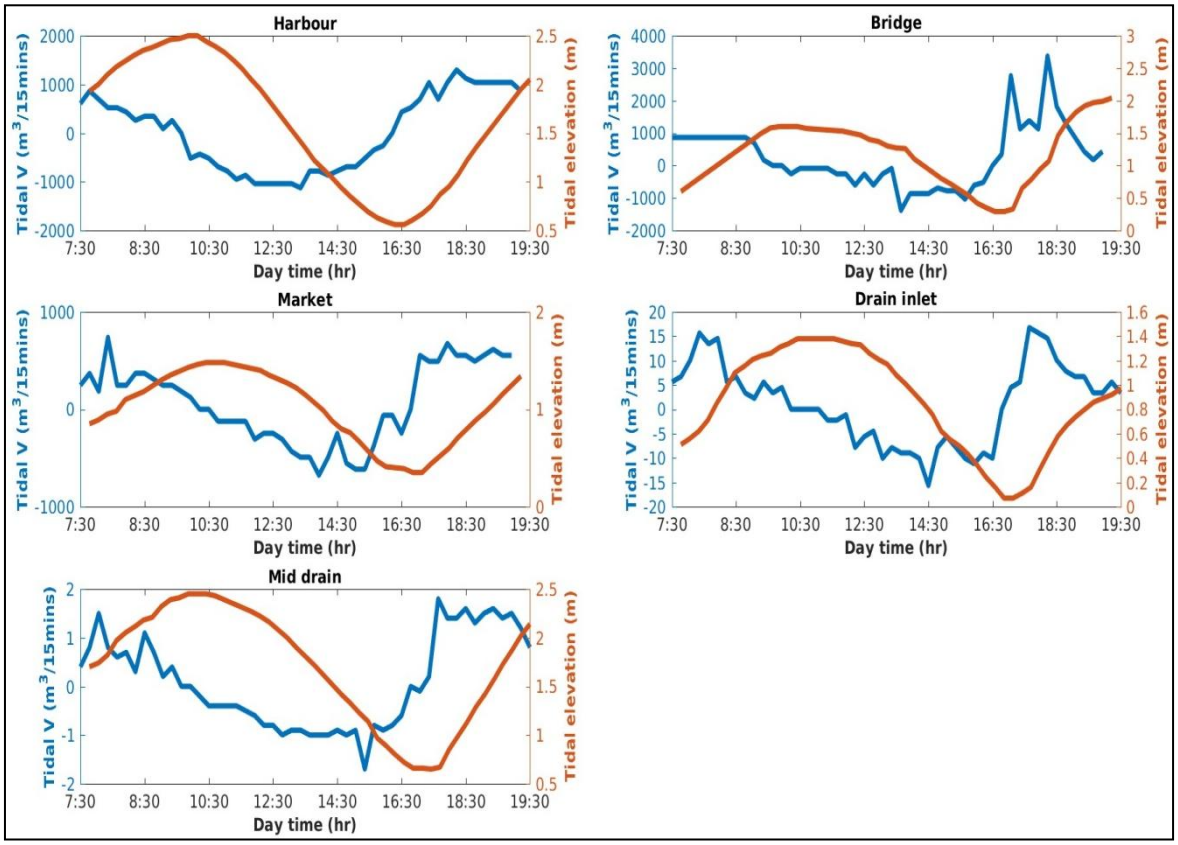

Fig. 7. Evolution of small-scale features of water discharge with alongside water level of neap tide condition. harbour, bridge, market, drain inlet and mid drain representing S0, S1, S2, S3 and S4 respectively

4.1 Tidal Signal

The results describing the tidal signal show that, during Spring conditions, the tidal amplitude obtained were 1.18, 1.23, 1.01, 0.96 and 1.18 m (Fig. 3B) representing the values in S0, S1, S2, S3 and S4 respectively. This spatial change in amplitudes (distortion) could be explained by the damping effect [30,31,13]. This damping trend has been reported by the latter authors to be related to change in estuary morphology (width and depth) and changing river flow. In the same sense. The hypersynchronous character observed from S3 (0.96 m) to S4 (1.18 m) could be explained by the rapid changes in cross-sectional area or funnel effect [32,13].

When comparing the two tidal conditions of this study, the relatively stronger amplitudes obtained during Spring tide are reduced during Neap tide periods (Table 2). The percentages decrease in each station were 13, 21, 28, 30 and 9.2% accounting for S0, S1, S2, S3 and S4 respectively. This differences in amplitudes between Spring and Neap tide conditions could be as a result of their different tidal coefficients; the tidal coefficient during Neap tide period was 56 and increases to 96 during Spring tide.

Finally, the semi-diurnal signal obtained in the Bessek's flood drain and it's surrounding Wouri estuary (Fig. 2A and B) confirms the results of [29,13,33] all working between the lower and the middle section of the Wouri estuary. This has been explained as a consequence of the domination of semi-diurnal components over diurnal species [13].

4.2 Evolution of Flow Velocity

During Spring situation, velocities decreases from S0 to S3, with values of 1.65, 1.50 and 1.40 m/s representing S0, S2 and S3 respectively (Fig. 4). In the same manner, the Neap tide trend is 1.38, 1.25, 0.9 and 0.8 m/s. These evolutions could be the effect of transition from tidal domination with lower fluvial influence (S0) to tidal domination with higher fluvial influences (S3) combined with a progressively reduced bathymetry (damping effect) [31]. The

unexpected high velocities (1.75 and 1.35 m/s for Spring and Neap respectively) obtained in the Mid drain section (S4) could be related to funnel effect. The flood drain acts as a sub estuary with hypersynchronous character. Similar results have been observed by Sandbach et al. [34] and were indorsed to funnel and resonance effect. The decreasing trend in tidal velocity observed from S1 to S3 during both tidal conditions portrays the hypo synthronus character while the amplification of velocity in S0-S1 and S3-S4 reflects a hypersynchronous character. According to Godin [35], tides amplifies as it enters into this estuary until a maximum amplitude is reached before being damped totally in the upper section of the flood drain. Base on the difference in water level, the tidal wave travel from S0 to S4 in about one (1) hour during spring tide and takes about 1h 30 mins to travel the same distance during Neap tide condition (Fig. 3A and B). This confirmed that Springtide has higher velocities than Neap tide conditions (Fig. 4). This differences in velocities between Spring and Neap tide could be explained by the fact that water particle travels faster when the depth increases.

4.3 Tidal Prism Evolution

The values of the tidal prism and associated parameters are presented in Table 1. It can be observed from this table that, The values of the various tidal parameters obtained during Spring tide conditions are relatively higher than their corresponding Neap tide values in all gauging station. Example, the tidal prisms crossing S0, S1, S2, S3 and S4 during Spring tide conditions are 2.1×10^4, 1.0×10^4, 1.3×10^4, 2.5×10^2 and 3.5×10^1 m^3 respectively (Table 2). When Comparing these values with their corresponding neap tide values, the percentage dropped were -19%, -31%, -38.5%, -48% and -48.6% in S0, S1, S2, S3 and S4 respectively. These differences in tidal prisms could be a result of tidal coefficients; the Spring condition with a tidal coefficient of 96 has greater amplitudes and is subjected to more intense tidal effects compared to the lower tidal coefficient of 56 in Neap tide. These tidal prisms are smaller than those obtained by several authors [19,36,27] working in the Lingdingyang Bay at pearl river Estuary, Venice Lagoon (Italy) and numerical models respectively. This situation could be explained by differences in the morphological parameters and distance of the experimental sites from the open ocean. For example, the Pearl River estuary appears to be larger than the Wouri estuary and consequently the Besseke's flood drain. The Venice Lagoon is found closer to the open ocean compared to the Wouri-Besseke estuary that is about 60km away from the open ocean. In the same way, the virtual site set up by Tran et al. [27] were located only 15 and 30 km away from the open ocean. This factors, therefore, have a strong influence on the hydrodynamic, hydrology and consequently tidal prisms of a tidally influenced estuary.

Looking at the spatial scale, Table 2 shows that the tidal range, discharge volume, cross-sectional area and tidal prism decreases from S0 to S4 for both tidal regimes. The tidal prisms crossing S0, S1, S2, S3 and S4 during Spring tide conditions were 2.1×10^4, 1.0×10^4, 1.3×10^4, 2.5×10^2 and 3.5×10^1 m^3 similarly, those of Neap tide were 1.7×10^4, 6.9×10^3, 8.0×10^3, 1.3×10^2 and 1.8×10^1 m^3 respectively. A comparable decreasing trend has been obtained in the Lingdingyang bay by Xu et al. [37] and was reported to be depending on the geometry of the basin in terms of surface area and mean water depth, the tidal range and to a lesser extent, freshwater inflow. Furthermore, the result obtained in section suggests that distance is an important parameter that affects tidal prism and could be taken into consideration in the designing and construction of flood drain or dykes in tidally influenced zones. The unregular high tidal prism found in S2 during both tidal conditions could be due to morphological parameters (bathymetry and cross-section length).

A strange situation was observed in Market (S2) in which higher tidal prism appear during Neap tide conditions. Similar cases have been illustrated by Terry and Charles [38] and Shigemura [39] working in New Zealand and Japan respectively.

4.4 Small Scale Features Dynamics

The tidal elevation and discharges volumes were extracted at the high-frequency sampling of 900 seconds (15 minutes). The aim here was to depict the dynamics in small-scale features of water discharges in the Bessek's flood drain and the surrounding environment. For comprehensive reasons, the tidal elevation and water discharges were plotted against time on the same curve.

Focusing on tidal elevation (Fig. 5), the small scale features observed during Spring tide conditions (red bars) have relatively higher amplitudes (stronger perturbation) compared to Neap tide conditions (blue bars). In the Besseke

middrain (S4) for example, the maximums amplitudes of elevations during flood/ebb currents were +0.21 -0.2 m in a Neap tide. These values increase to + 0.25 m and -0.3 m during flood and ebb currents of Spring tide conditions. This differences in intensities between the two tidal regimes can be explained from their differents tidal coefficients. The maximum amplitudes of small-scales tidal dynamics appeared around 04:30 pm and 06:30 PM, during Spring and Neap tide respectively, this occurrence was found to coincide with the near high waterslake period of both conditions. The spatial trend in these peaks values was Bridge (S1) > Mid drain (S4) > Harbour (S0) > Market (S2) > Drain inlet (S3). This trend is different from that observed in Tidal prism (Table 2). This difference could be due to their weather effects; strong short life winds could cause strong amplification (peaks) within a small time scale, this effect could be hidden in the long term especially if the wind stress stop. The unexpected strong dynamics in the Besseke's drain could be related to it sub estuarine nature.

Looking at Small scale features of tidal discharge or flow presented in Figs. 6 and 7, a decreasing trend was observed from S0 to S4 (i.e Harbour > Bridge > Market > Drain inlet > Mid drain) during both tidal regimes. The estimated peaks values obtained during flood tide of Spring conditions (Fig. 6) were 1800, 1500, 1000, 20 and 05 m^3/15mins while those for the flood tide in Neap regime (Fig. 7) were 1000, 3000, 900, 17 and 02 m^3/15mins respectively for S0 (Harbour), S1 (Bridge), S2 (Market), S3 (Drain inlet) and S4 (Mid drain). inversely, the volume of water that left these stations during the ebb tide of spring condition were -1000, -500, -700, -21 and -2.1 m^3/15 mins. These values reduce to -1000, -900, -500, -17 and -02 m^3/15 mins during the ebb of the neap tidal regime. The small scale features observed in spring tide regime (Fig. 6) were more intense than those observed during the neap tide condition (Fig. 7). The difference in small-scale discharges between these two inter regime conditions could be explained by their tidal coefficients and weather conditions (i.e. winds stress only since no rain was reported in the nearby environment during the sampling periods). The presence of wind in the direction of flow can cause surges tides explaining the various peaks. These results also showed that the study ground is a flood dominated area; water enters quickly and goes out slowly. This dynamic could be responsible for the daily filling observed in the Besseke's flood drain (S4). The temporal dynamics of these small-scale features in flow reveals that the peak values appear between 02:30 – 03:00 pm (14:30-15:00) during spring tide and from 05:00 - 18:30 (17:00–18:30) during neap tide regime (Figs. 6 and 7). These periods correspond to one (01) hour before high water slake. Oppositely, the emptying is more intense during the last hour before low water slakes, i.e. around 10:30 am in spring and 02:30 pm during the neap tidal condition. This results also concluded that during low or high water slake, the dynamics in small scales features of flow are not stable as expected. These instabilities could be attributed to weather effects.

4.5 Relationship between Cross-sectional Area and Tidal Prism (A-P relation-ship)

A relationship between cross-sectional area (A) and tidal prism (P) was established following the method developed by O'Brien [23]. The results of this empirical relation were presented in Fig. 8. A perfect correlation (r^2 = 0.96) was obtained between these two parameters, indicating that they are directly related. [21,23,24,40,26,27] working in different estuaries and inlets, obtained correlations ranging within the same order ($0.95 \leq r^2 \leq 0.98$). The coefficients **a** and **n** computed from this relationship (3.40×10^{-2} and 0.46 respectively) are in the range of those obtained by Powell et al. [28] for medium longshore transport systems, where **a** = 1.2×10^{-2} and **n** = 0.69. This result confirms that these two parameters are inter-independent and change in the value one will directly affect the other. However, deviations from O'Brien's relationship (blue line) were observed around some points. This result was similar to that obtained by [41]. According to this author, the differences between the predicted and observed values of the tidal prism and cross-sectional area are due to topography, confluence effect and drying or wetting processes affecting the littoral drift, tidal periods, river flow and grain diameter. These factors, therefore, have to be taken into consideration during the designing and construction operations of flood drains around the Besseke's neighbourhoods. Furthermore, the qualitative analysis of these deviations inferred either erosional or depositional processes (Fig. 8).

Erosional processes were observed in the Drain inlet (S3) and Mid drain (S4) sections during both

tidal regimes. This process again encountered in the Bridge (S1) and Harbour (S0), but in this case only during Spring regime. Many authors founded similar situations and according to these references, the erosion experience here could be explained from the fact that the tidal prism that passed through these sections were greater than equilibrium cross-sectional area, resulting in erosion [36]. This situation could even be exacerbated by the presence of an alongshore drift that may yield a reduction of about 30% in the cross-section [17]. According to these explanations, the relatively higher tidal prism passing the Besseke's flood drain could be responsible for its daily filling and aggravated by the low altitude of the besseke neighbourhood. This altitude has been reported to be oscillating between 0.00 and 1.25 m [11].

The deposition process was presented by an upward deviation (Fig. 8). This situation was observed in the Harbour (S0), Bridge (S1) and Market (S3) principally during Neap tide. Paradoxically to the erosional processes, this condition arrived from the relatively lower tidal prism compare to the equilibrium cross-section. Antagonistic to erosional processes, the fall in intensity of alongshore drift could increase the deposition rate.

The best-fitted relationship observed in the Market (S2) showed that the tidal prism/cross-sectional area were in equilibrium with that predicted during both tidal conditions. In this station, the tidal prism and cross-sectional area were in a steady-state without erosion or deposition processes. This means that a more accurate tidal prism could be estimated from the cross-sectional area and vice versa. The drain project could, therefore, be more efficient in this section.

4.6 Stability of the Besseke Neighbourhood

The stability of a tidal influence zone can be evaluated upon application of tidal prism/cross-sectional area relationship [29]. In Fig. 8, Stations having a smaller cross-section or large tidal prism than the relationship predicted revealed that the inlets/station will erode the cross-sectional area to accommodate the tidal prism [36]. This was the case in the Drain inlet (S3) and Mid drain (S4) during both tidal regimes. An opposite situation was reported during the Neap tide in the Market (S2) and Harbour (S0) section. The former was again founded to be in perfect equilibrium during Spring tide condition. At this point, the cross-section can increase with erosion or decrease with deposition, this will eventually affect the discharge and velocity rate which will consequently stabilize the tidal prism and cross-section in case of any change. If the cross sectional/tidal prism relationship is in equilibrium, the inlet should be self dredging as the width is fixed.

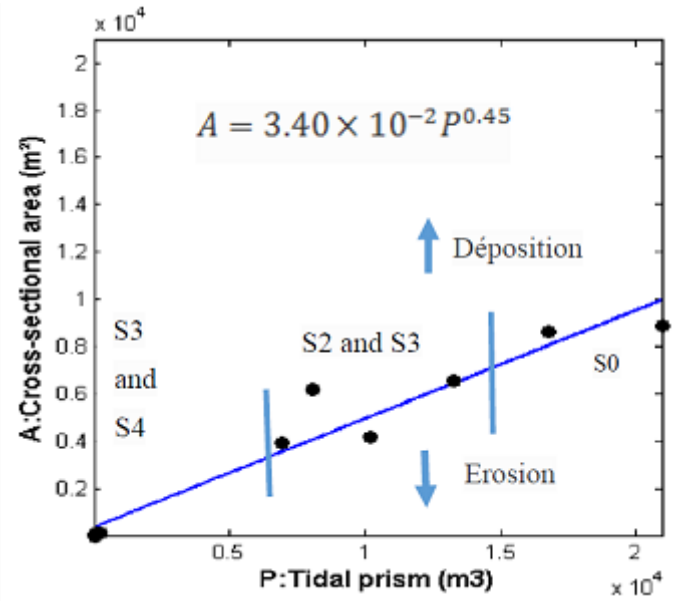

Fig. 8. Relationship between cross-sectional area (A) and the related tidal prism (P) for the various sampling stations along the Besseke flood drain and the Wouri estuary. The continuous line portrays the O'Brien-Jarret relationship with a = 3.40 ×10^{-2} and n = 0.46

4.7 Dilution/mixing in the Besseke's Flood Drain

The salt fraction of the water in the midrain portion (S4) was estimated to understand the origin of the water filling the drain. The results of this estimate are presented in Table 3. It is observed that the fraction of brackish water in the Besseke's flood drain changes from 85.7% in Spring tide to 77.8% during Neap tide (Table 3). Inversely, the freshwater fraction changes from 14.29% in spring to 22.2% during the Neap tidal regime. This antagonistic evolution of brackish-fresh water fraction in the flood drain could be due to the differences in tidal coefficients. Springtide with a greater tidal coefficient (96) brings larger volumes of brackish water in the Besseke's flood drain compared to the neap tide (56) conditions. A large amount of brackish water that penetrates the mid drain of Besseke during Spring conditions will easily overcome the freshwater from urbanisation.

5. CONCLUSION AND RECOMMENDATIONS

This paper aims to examine the dynamics of small scales tidal parameters along the Besseke's flood drain and the surrounding Wouri estuary, to mitigate daily flood events. To succeed in this task, five (05) sampling stations were installed along the Wouri Estuary and the Besseke's floodrain (Fig. 1). The data obtained during the two distinct periods with tidal coefficients of 56 (Neap tide) and 96 (Springtide) of May 2019 were analyzed. The results show that small scale dynamics observed in the Spring tide regime are more intense than those observed during the Neap tide condition. This analysis has, therefore, provide evidence of surges tides with low intensities and consequently marine submersions along the Besseke flood drain with an amplification during Spring conditions. Looking at the spatial evolution, the trend in tidal prism was Harbour > Market > Bridge > Drain inlet > mid drain with corresponding values of 2.1×10^{4}, 1.0×10^{4}, 1.3×10^{4}, 2.5×10^{2} and 3.5×10^{1} m^3 respectively. Focusing on the percentage composition of water volume in the Mid drain (S4) only, the fraction of brackish water in the Besseke flood drain changes from 85.7% in Spring tide to 77.8% during Neap tide. Inversely, the freshwater fraction changes from 14.29% in Spring to 22.2% during the Neap tidal regime. Tidal prism and Cross-sectional area shows a perfect correlation (r^2 = 0.96). The results of this study also concluded that data from S2 best fitted the relation of O'Brien compared to S0, S1, S3 and S4. The deviation in S3 and S4 could be attributed to topography, confluence effect drying or wetting processes and possible alongshore drift. It is therefore important to consider these parameters before any engineering activity related to flood management in the Besseke's neighbourhood.

The results of this study open perspectives for future research work promising on both apply and fundamental sciences. These recommendations are :

- The installation of a weather station that will evaluate the atmospheric contribution in the daily flooding of the Besseke's flood drain and the surrounding environment ;
- The comprehension of sediment transports mechanisms should also be conducted in this zone to understand sand filling of the Drain;
- The application of the O'Brien formula (equation 6) at different time scale including seasonal level to have a more realistic equilibrium between cross-sectional area and a tidal prism that will properly be used for the sustainable construction of flood prevention infrastructures;
- The model should be developed that will ease the validation of an alert system to anticipate flood events. Intense fieldwork is required for this.

ACKNOWLEDGEMENT

The field work of this research was supported by the Department of Oceanography of the Institute of Fisheries and Aquatic Sciences of the University of Douala, the authors are grateful for the instruments given to them during field operations. Special thanks to Mr. LANGOUL Ulrich for his contributions. Particular thanks goes to the Association for Nature Conservation (ASCON) for the active participation during data collection.

COMPETING INTERESTS

Authors have declared that no competing interests exist.

REFERENCES

1. Grigg Neil S, Rice Leonard R, Bothan Leslie H, Shoemaker WJ. Evaluation and

implimantation of urban drainage and flood control projects. Completion report series 056, OWRR Project number B.08-COLO. 1974;145.
2. Resio DT, Westerink JJ. Modeling the physics of storm surges, Phys. 2008; 61:38.
DOI: 10.1063/1.2982120
3. Pugh DT, Wiley J, Chichester and Sons. Tides, Surges, Mean Sea-Level. A handbook for engineers and scientiste. 1987;472.
4. Zheng F, Westra S, Sisson SA. Quantifying the dependence between extreme rainfall and storm surge in coastalzones, J. Hydrol. 2013;505:187.
DOI:10.1016/j.jhydrol. 09.054.
5. Torres JM, Bass B, Irza N, Fang Z, Proft J, Dawson C, Kiani M, Bedient P. Characterizing the hydraulic interactions of hurricane storm surge and rainfall – runoff for the Houston – Galveston region, Coast. Eng. 2015;106:19.
6. Olbert A, Comer J, Nash S, Hartnett M. High-resolution multi-scale modeling of coastal flooding due to tides, storm surges and rivers inflows. In Cork City example, Coast. Eng. 2017;121:278-297.
Available:https://doi.org/10.1016/j.coastaleng.2016.12.006
7. Leone F, Meschinet de richemond N, Vinet F. Natural hazards and risk management, Paris - PUF. 2010;287.
8. Ngo-Tu. Environmental assessment of the risk of flooding in the Ha Thanh river delta (central Viet-Nam). University of Orlans, Doctoral School of Man and Society, CEDETE Laboratory. 2014; EA1210:316.
9. Olinga OJM. Vulnerability of urban spaces and local strategies for sustainable development. Case study of the city of DOUALA (Cameroon). Douala (CMR): Research Laboratory. Planning and Sustainable Development-UDla. 2011;161.
10. Munji CA, Mekou YB, Monica E, Idinoba,, Denis JS. Floods and mangrove forests, friends or foes? Perceptions of relationships and risks in Cameroon coastal mangroves, Estuarine, Coastal and Shelf Science. 2013;140:75.
11. Feumba R. Hydrology and evaluation of the vulnerability of aquifers in the Besseke watershed (Douala, Cameroon), These presented and supported with a view to obtaining a Doctorate / PhD. In Earth Sciences, Option: Geology of superficial formations, Laboratory of Engineering Geology and Alterology, University of Yde I. 2015;277.
12. Sonè Essoh Willy. Mapping of areas at risk of flooding in the Tongo-Bassa watershed in Douala. Research Master thesis in Environmental and Fisheries Resources Management. Doctoral School of Basic and Applied Sciences of the University of Douala, Cameroon. 2018;73.
13. Onguéné R, Penha J, Dupehait Y, Esturnel C, Marsaleix P, Duhaut T. Overview of tide characteristics in Cameroon coastal areas using recent observations. Open Journal of Marine Science. 2014;5:13.
Available:http://dx.doi.org/10.4236/ojms.2015.51008
14. Kana TW, Hayter EJ, Work PA. Mesoscale sediment transport at southeastern U.S. tidal inlets: Conceptual model applicable to mixed energy settings. Journal of Coastal Research. 1999;15(2):313.
15. Olivry JC, Hoorelbecke R, Andiga J. Quelques mesures complémentaires de transports solides en suspension au Cameroun. Technical Report, Orstom, Yaounde; 1974.
16. Olivry JC. Fleuves et rivières du Cameroun. Monographies hydrologiques ORSTOM. 1986;9.
17. Marcel SJF, Rakhorst RD. Review of empirical relationships between inlet cross-section and tidal prism. Journal of Water Resources and Environmental Engineering. 2008;23:08.
18. Hume TM, Schwartz M. Tidal prism (eds) Encyclopedia of Coastal Science. Encyclopedia of Earth Science Series. Springer, Dordrecht. 2005;1197.
19. Shenguang F. Analysis of tidal prism evolution and characteristics of the Lingdinyang Bay at Pear river estuary. 2015;10.
20. Seaburgh. Hydynamics of tidal inlets. Coastal engineering manual. US Army corps of engineerings, Washintong D.C. 2002;79.
21. Leconte LJ. Discussion of Notes on the Improvement of River and Harbor Outlets in the United States Paper No. 1009 by D.A. Watts, Transactions, American Society of Civil Engineers, LV. De.1905; 308.
22. O'Brien M P. Estuary tidal prisms related to entrance areas. Civil Engineering. 1931; 1(8):739.

23. O'Brien MP. Equilibrium flow areas of inlets on sandy coasts. Journal Waterways and Harbors Division, New York. ASCE. 1969;52.
24. Jarrett JT. Tidal prism-inlet area relationships. Fort Belvoir, Virginia and Vicksburg, Mississippi: U.S. Army Corps of Engineers, Coastal Engineering Center and Waterways Experiment Station, GITI Report #3. 1976;76.
25. Thomas L, Tandon A, Mahadevan A. Submesoscale processes and dynamics. In M.W.Hetch and H.Hasumi (Eds.), Ocean modelling in an eddying regime, Geophysicacl monograph series. American Geophysical Union, Washington DC. 2008;177:38.
26. Marcel JF, Stive, Liang Ji, Ronald L. Brouwer, J. (co) Van de Kreeke and Roshanka Ranasinghe. Empirical relation-ship between inlet cross-section and tidal prism: A Re-evaluation. 2010;10.
27. Tran TT, Jacobus VK, Marcel JFS, Dirk-Jan RW. Cross-sectional stability of tidal inlets: A comparison between nu,erical and empirical approaches. Journal of Coastal Engineering.Coastal Engineering. 2012; 60:21-29.
28. Powell MA, Thieke RJ, Mehta AJ. Morphodynamic relationships for ebb and flood delta volumes at Florida's entrances. Ocean Dynamics. 2006;307.
29. Heath RA. Stability of some New Zealand coastal inlets. New Zealand Journal of Marine and Freshwater Research. 1975;9: 459.
30. Koutitonsky V. Oceanographic sensors for the system of environmental monitoring of the Autonomous Harbour of Douala. Technical report, Hydrosoft SA. 2005;63.
DOI: 10.13140/2.1.2678.0969
31. Matte P, Secretan Y, Morlin J. Temporal and spatial variability of tidal-fluvial dynamics in the St Lawrence fluvial estuary: An application of nonstatioary analysis. Jornal of Geophysical Researche: Oceans. 2014;119.
DOI: 101002/2014JC009791
32. Le Floch JF. Propagation of the tide in the Seine estuary and in Seine-Maritime. Thesis from the University of Paris. 1961; 507.
33. Kouandji BJB. Coastal ocean dynamics of the Gulf of Guinea by 3D modeling. European University Editions. International Market Service Book. Ltd. 2018;37.
[ISBN: 978-620-2-28394-6]
34. Sandbach SD, Nicholas AP, Ashworth PJ, Best JL, Keevil CE, Parsons DR, Prokocki EW, Simpson CJ. Hydrodynamic modelling of tidal-fluvial flows in a large river estuary. Estuarine, Coastal and Shelf Science. 2018;212:188.
35. Godin G. The propagation of tides up rivers with special considerations on the Upper Saint Lawrence River, Estuarine Coastal Shelf Sci. 1999;48(3):324.
36. Helsby R, Carl Amos L, Georg Umgiesser. Tidal prism variation and associated channel stability in the N Venice Lagoon. Scientific Research and safeguarding of Venice, Edition: 2008;4:466.
37. Xu FJ, Zhu SK, Wang H. Analysis of Hydrodynamic Environment of Lingdingyang Bay and Improvement Strategy. Pearl River (in Chinese). 2004; (1):14.
38. Terry M. Hume, Charles E. Herdendorf. The "Furkert-Heath" relationship for tidal inlet stability reviewed, New Zealand Journal of Marine and Freshwater Research. 1988;22(1):134.
DOI:10.1080/00288330.1988.9516284
39. Shigemura T. Tidal prism-throat area relationships of the bays of Japan. Shore and Beach. 1980;48(3):35.
40. Van de Kreeke J. Adaptation of the Frisian inlet to a reduction in basin area with special reference to the cross-sectional area of the inlet channel. In Dronkers, J. and Scheffers, M.B.A.M. (Eds). Proc. PECS Conference. 1998;362.
41. D'Alpaos A, Lanzoni S, Marani M, Rinaldo A. On the tidal prism–channel area relations, J. Geophys. Res. F01003. 2010; 115.
DOI:10.1029/2008JF001243

Peer-review history:
The peer review history for this paper can be accessed here:
http://www.sdiarticle4.com/review-history/54504